CrossMark

ARTICLE

Carbon black dispersions in surfactant-based microemulsion

Mohamed Youssry[a)]
Department of Chemistry and Earth Sciences, College of Arts and Sciences, Qatar University, Doha 2713, Qatar

Dominique Guyomard and Bernard Lestriez
Institut des Matériaux Jean Rouxel, Centre National de la Recherche Scientifique (CNRS), Université de Nantes, Nantes Cedex 3 44322, France

(Received 1 October 2017; accepted 16 November 2017)

In an attempt to introduce a novel approach to formulate carbon black (ketjen black) suspension with enhanced colloidal stability, improved flowability, and higher conductivity, ketjen black was dispersed in microemulsion systems composed of a non-ionic surfactant (Triton X100), decanol, and water. Rheo-electric and rheo-microscopy proved to be very powerful techniques that are able to elucidate the microstructure evolution with the composition and under shear flow. Interestingly, the carbon black slurries at low decanol/water ratio are weak gels (flowable) with higher electrical conductivity than those at higher ratio, which shows strong-gel viscoelastic response. In addition, the slurries show recoverable electrical behavior under shear flow in tandem with the viscosity trend. It is likely that the oil-in-water microemulsion enhances slurries' stability without affecting the percolating network of carbon black. On the other hand, the oil-in-water analogous and bilayer structure of the lamellar phase makes the slurries less conductive as a consequence of losing the network percolation.

I. INTRODUCTION

To enhance the energy and power densities of electrodes for energy storage systems, the formulation and processing of electrode slurries proved to be a critical issue in determining the electrode performance. Carbonaceous materials such as carbon black (CB), nanotubes, and nanofibers are main conductive additives in the electrode slurries.[1,2] These materials are characterized by exceptional chemical stability and electrical and mechanical properties derived from their large diversity of structure that extends from the sp^2-hybridization of carbon atoms to the crystalline structure (degree of graphitization). Among various kinds of carbonaceous materials, semispherical (three-dimensional) CB has a unique place in the formulations of electrodes for energy storage systems.[3,4]

CB is initially formed from semispherical primary particles of nanometric (few hundred nm) size, which are fused to form aggregates (few μm size scale) in suspensions. The van der Waals attraction forces drive the aggregates to bind into larger loosely agglomerates (10–100 μm).[5] The surface area and surface chemistry of CB play a pivotal role in determining the strength of binding forces[6] which determines the microstructure and hence the flow behavior of CB suspensions.[7] Above a critical concentration, the so-called percolation threshold, a three-dimensional network is formed across the CB suspension showing abrupt increase of the rheological parameters (viscosity, shear modulus, and yield stress) and electrical conductivity of the suspension.[5,8] This behavior is a consequence of formation of the percolated network composed of branches (paths) of aggregated CB resulting in a 3D network.[5] It has been reported that the particle size of CB impacts on their rheological behavior where large particles form a weaker percolated network consisting of less dense agglomerates with numerous branches and hence lower rheological parameters and electrical conductivity.[5] Of course, the surface chemistry of CB, dispersion medium, and dissolved salt (type and concentration) might influence the rheological and electrical behaviors of CB suspensions. Nevertheless, no systematic study has been appeared so far, addressing the influence of such parameters on the properties of CB suspensions. Such a study is mandatory since CB is the conductive additive used in commercial energy storage systems such as lithium-ion batteries (at a concentration of approximately 2 wt%).

Commonly, electrode slurries are prepared in organic electrolytes due to the compatibility with the highly hydrophobic solid materials, especially CB. Recently, the organic electrolyte was replaced by an aqueous-based one,[9,10] but the limited cell voltage remained an obstacle toward commercial applications. The advantages of aqueous electrolytes, such as environmentally friendly, highly safe, low viscosity, etc., challenge us to examine the replacement of some amount of water by an organic

Contributing Editor: Yat Li
[a)]Address all correspondence to this author.
e-mail: myoussry@qu.edu.qa
DOI: 10.1557/jmr.2017.451

 © Materials Research Society 2017

https://doi.org/10.1557/jmr.2017.451 Published online by Cambridge University Press

solvent in the presence of a nonionic surfactant (Triton X100) which is commonly used in the formulation of electrode slurries.[11] At specific composition, this novel electrolyte is the microemulsion.

Microemulsions are transparent thermodynamically stable fluids made up, essentially, of surfactants, oil, and water and sometimes cosurfactants (such as medium chain length alcohols).[12,13] Their formation is entropy-driven, and thus it is quite different from coarse emulsions.[14] Depending on the concentration, temperature, and salinity (for ionic surfactants), they may be Winsor I (oil-in-water; O/W microemulsion), Winsor II (water-in-oil; W/O microemulsion), or Winsor III (bicontinuous microemulsion).[15] Both Winsor I and II microemulsions contain isolated aggregates (droplets) of a typical size of 10–100 nm, and they are called swollen micelles. On the other hand, Winsor III (bicontinuous) microemulsion has continuous water and oil phases. O/W and bicontinuous microemulsions have nearly similar conductivity to that of homogenous aqueous electrolyte solutions; therefore, they were used for electrochemical studies.[16,17]

In this study, we attempt to study the microstructure and shear-induced transitions for a percolated dispersion of CB at 2 wt% in a microemulsion system composed of Triton X100, decanol, and water.[18]

II. EXPERIMENTAL

A. Materials and samples preparation

Ketjen black EC-300 (KB, density = 1.90 g/cm^3, BET [Brunauer-Emmett-Teller] surface area = 800 m^2/g^1) was purchased from Akzo-Nobel (Sundsvall, Sweden), Triton X100 (*t*-octylphenoxypolyethoxyethanol; average molecular weight = 625 amu, critical micelle concentration, cmc = 0.9 mM at 25 °C, with a cloud point = 65 °C), and 1-decanol (99%) was obtained from Sigma Aldrich (Saint-Quentin-Fallavier, France). Distilled water was used in the preparation of samples.

First, selected microemulsion systems along four dilution lines [Fig. 1] were prepared by stirring an appropriate amount of Triton X100 with decanol and distilled water. Table I depicts the composition (in weight-by-weight percentage w/w) of the microemulsions used in this study.

The KB suspensions were prepared by mixing a fixed amount (at 2% w/w) of KB with the microemulsions by using a planetary ball-mill (Planetary Micro Mill PULVERISETTE 7 classic line, FRITSCH, Idar-Oberstein, Germany) at 500 rpm for one hour at ambient temperature.

B. Rheo-dielectric measurements

In a stress-controlled rotational rheometer (Physica MCR 101, Anton Paar, Courtaboeuf, France) the dynamic and steady shear rheological measurements were conducted

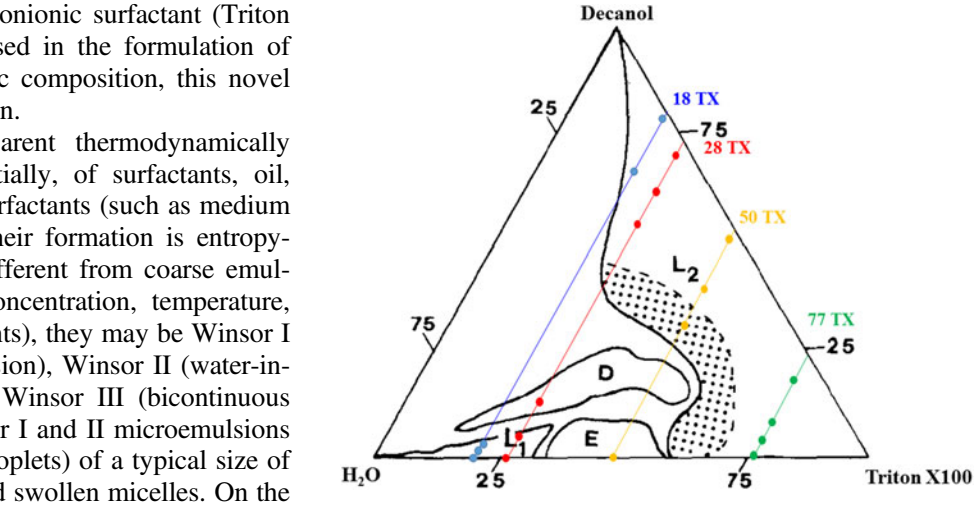


FIG. 1. Ternary phase diagram of Triton X100–decanol–water at 20 °C. Reproduced with permission from Ref. 18. The colored lines are the four dilution lines at 18, 28, 50, and 77 wt% Triton X100.

TABLE I. Composition of microemulsions in weight/weight percentage and the corresponding phase type.

Phase	Triton X100 (wt%)	Decanol (wt%)	H_2O (wt%)	Decanol/H_2O ratio
		0	82	0
L_1		1	81	0.012
	18	2	80	0.025
		65	17	3.8
L_2		81	1	81
		2	70	0.030
L_1		4	68	0.060
L_α		16	56	0.29
	28	52	20	2.6
L_2		62	10	6.2
		67	5	13.4
		28	22	1.3
L_2	50	38	12	3.2
		48	2	24
		0	23	0
		5	18	0.30
L_2	77	10	13	0.77
		20	3	6.7

at 25 C using a plate–plate geometry with a plate diameter of 50 mm and a gap of 1 mm. The electrochemical impedance spectra represented by Nyquist plots were simultaneously recorded under shear flow using a potentiostat/galvanostat (SP200, Bio-Logic Science Intruments, Seyssinet-Pariset, France) connected to the rheometer.

To avoid the effect of aging on the rheological and electrical behaviors, the freshly prepared KB suspensions were directly examined. The samples were first pre-sheared at 100 s^{-1} for 10 min to eliminate the shear history and guarantee a similar treatment for all samples. Then, the samples were left for 5 min at rest to recover the equilibrium structure.

https://doi.org/10.1557/jmr.2017.451 Published online by Cambridge University Press

The impedance spectra were recorded over a frequency range of 10^{-2}–10^{5} Hz with an ac of amplitude = 100 mV. The impedance spectra under flow conditions were recorded at the end of each shear flow sessions (15–30 min) where the steady shear conditions were almost achieved.

C. Rheo-microscopy

The optical inspection of the samples was done using the optical shear system (CC450, Linkam, Tadworth, United Kingdom). The samples were placed between two polished quartz plates at 1 mm gap and 25 °C. The photographs were recorded using a CCD (charged couple device) camera at defined shear rate.

III. RESULTS AND DISCUSSION

A. The phase diagram of Triton X100–decanol–water system

Figure 1 represents the phase diagram of the Triton X100–decanol–water system at 20 °C.[18] The authors described the phase diagram to be dominated by a very large region of an isotropic reverse micellar solution (denoted by L_2) at the Triton–decanol corner and a small direct micellar region (L_1) in the water-rich part. The two micellar phases are separated by two lyotropic liquid crystalline phases: lamellar (L_α) and hexagonal (E) phases. Nevertheless, the isotropic phases are not usual micellar systems, instead they are microemulsion systems. The L_1 phase is an oil-in-water (O/W) microemulsion (Winsor I), but the L_2 phase is a water-in-oil (W/O) microemulsion (Winsor II).

B. Rheology of microemulsions

The rheological properties of microemulsions reflect the evolution of microstructure from discontinuous to bicontinuous microemulsion. By comparison, Fig. 2 demonstrates the dynamic frequency sweep [Fig. 2(a)] and steady shear rheology [Fig. 2(b)] for two microemulsions in L_1 and L_2 phases at constant surfactant concentration (28 wt%). It can be seen that both O/W and W/O microemulsions show a liquid-like rheogram where the loss modulus (G') is higher than the storage modulus (G'') and both dynamic moduli are somewhat dependent on the angular frequency (ω). Moreover, the magnitude of the dynamic moduli of the O/W microemulsion is slightly higher than those of the W/O microemulsion [Fig. 2(a)]. Rationally, the W/O microemulsion exhibits a pure Newtonian behavior where the steady shear viscosity (η) is independent of the shear rate [Fig. 2(b)]. This is in accordance with the behavior exhibited by discontinuous O/W microemulsions of analogous surfactant/oil/water systems.[19] However, the W/O microemulsion exhibits a weak shear-thinning behavior at low shear rates and becomes Newtonian at higher shear rates [Fig. 2(b)]. This behavior is in contrast to previous studies that showed shear-thinning only at very high shear rates.[20,21] Such a discrepancy may attribute to probable weak interaction between the clustered droplets of the percolating microemulsion so that they rearrange under low shear rates. It should be stated that the rheology of microemulsion systems is strongly influenced by the type, morphology, and degree of clustering of droplets as well as the interaction between droplets. However, rheology is not sensitive enough to elucidate the shear-induced microstructure encountered in microemulsions.

C. Dispersions of CB in microemulsions: equilibrium microstructure

CB is the common electrically conductive additive in the formulation of electrode slurries in rechargeable and semisolid redox batteries. It lends the electrical conduction when a three-dimensional network is constructed above a critical concentration, the so-called percolating threshold where the pathways (branches) are fully built through the dispersion. Conductive KB is a highly conductive commercial type of CB that has a percolating threshold at 2 wt% in organic[5] and aqueous[22] media. Accordingly, 2 wt% KB was selected in the current study to examine its dispersion in microemulsion systems. Along the four dilution lines [Fig. 1], various dispersions of KB in L_1 and L_2 phases were prepared and examined by rheology, impedance spectroscopy, and optical inspection under flow conditions. The detailed composition of various dispersions is depicted in Table I.

To assure the minimal perturbation for the microstructure of the KB dispersions, the linear viscoelastic regimes were identified by the dynamic strain sweep tests (data not shown). In general, the dispersions show a gel-like response where the storage modulus (G') is higher than the loss modulus (G'') and both moduli are independent of the strain at low strain amplitude. This is the linear viscoelastic region above which the G'–G'' crossover appears and G' becomes lower than G'' where the dispersions behave liquid-like indicating the serious perturbation of the microstructure.

Figure 3 depicts the dynamic frequency sweep tests for dispersions of 2 wt% KB in various microemulsions along the four dilution lines. This is a dynamic rheology where the flow is induced by applying the pre-defined (from strain sweep experiments) minimal strain amplitude, and the variation of dynamic moduli (G', G'') is monitored with the angular frequency (ω).

It can be seen from Fig. 3 that all the KB dispersions present a weak gel-like rheological response where G' is one decade higher than G'', and G'' shows some dependency on the frequency until the moduli crossover at higher frequency. This qualitative description reveals the

https://doi.org/10.1557/jmr.2017.451 Published online by Cambridge University Press

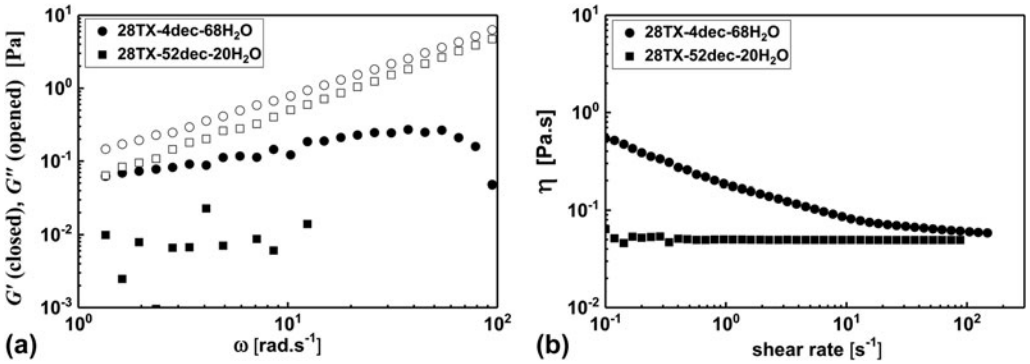


FIG. 2. (a) Dynamic frequency sweep tests and (b) steady shear rheology of two samples in the L_1-phase (O/W microemulsion) at 28 wt% Trion X100-4 wt% decanol–68 wt% H_2O and L_2-phase (W/O microemulsion) at 28 wt% Trion X100-52 wt% decanol–20 wt% H_2O.

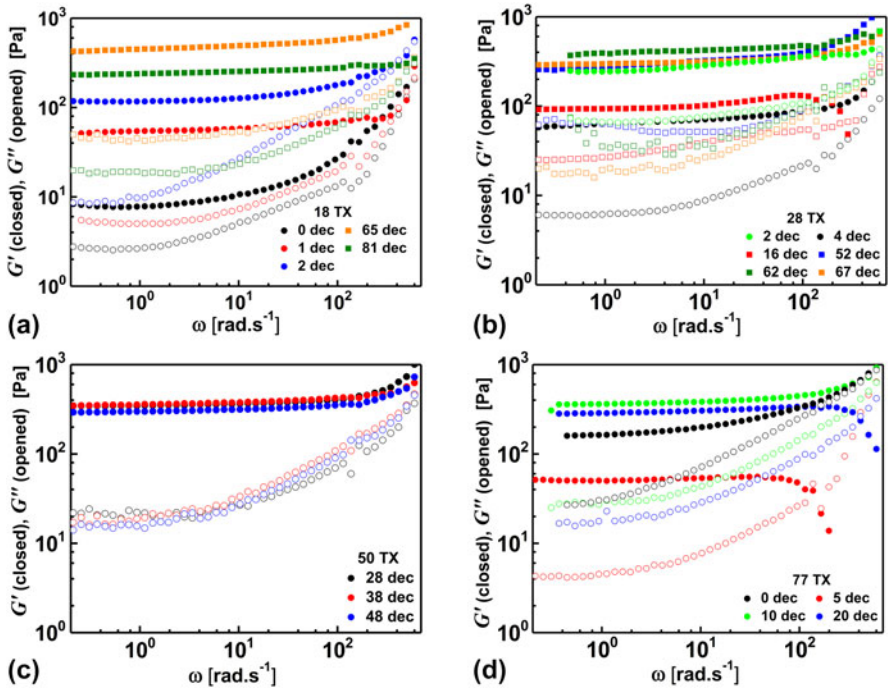


FIG. 3. Variation of storage (G') and loss (G'') moduli with the angular frequency (ω) for carbon black dispersions at 2 wt% KB in various microemulsion systems (L_1: circles and L_2: squares). The composition of the microemulsion is represented by wt% (e.g., 18 TX 1 dec denotes 18 wt% Triton X100, 1 wt% decanol, and 81 wt% H_2O).

percolated nature of the KB dispersions, but the density of KB branches is not high enough to form a strong gel. It is worth noting that the KB dispersions in L_1 microemulsions (circles in Fig. 3) have lower magnitudes of dynamic moduli than their analogous prepared in L_2 microemulsions (squares in Fig. 3). This trend is independent of the concentration of the surfactant. Moreover, the magnitudes of G' and G'' for KB dispersions in the L_1 phase are strongly influenced by the decanol/water ratio [Fig. 3(a)] much more than those prepared in the L_2 phase [Fig. 3]. In general, the dispersions of 2 wt% KB in microemulsions exhibit a weaker gel-like rheological response and lower magnitude of dynamic moduli than the dispersion of 2 wt% KB in pure Triton X100 (at only 5 wt% Triton).[11]

To quantitatively account for the effect of decanol/water ratio on the rheological behavior of the dispersions, the variation of the plateau modulus (G_0) with decanol/water ratio is depicted in Fig. 4. At very low decanol/water ratios (<0.03), the L_1-based KB dispersions are very sensitive to decanol addition and G_0 strongly increases. Above a ratio of 0.03, G_0 abruptly decreases again. This behavior may be ascribed to a structural transition from normal micelles, over a very limited region, to O/W microemulsions that stabilize the KB dispersion. The inset micrograph (left) reveals the

https://doi.org/10.1557/jmr.2017.451 Published online by Cambridge University Press

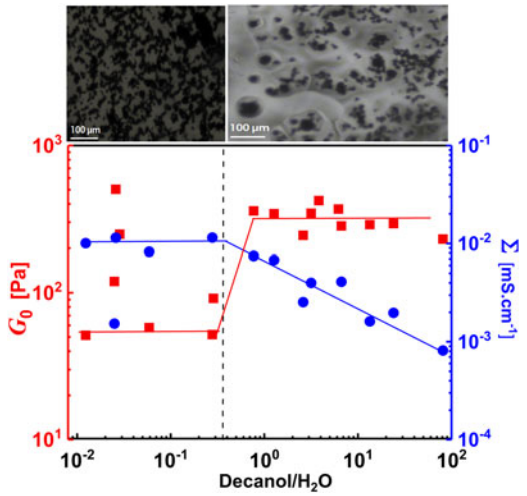


FIG. 4. Variation of the rheological plateau modulus (G_0) and electrical conductivity (Σ) with the decanol/H_2O ratio. The solid lines are a guide to the eyes, and the dashed line separates the KB dispersions in L_1 and L_2 microemulsions. The inset photographs are KB dispersions in L_1 (left) and L_2 (right) phases. Using EC-Labs software (Bio-Logic Science-Instruments), the Nyquist plots [Fig. 5] were fitted by an equivalent circuit proposed in Ref. 5 to obtain the electrical conductivity of dispersions.

microstructure of the KB dispersion at equilibrium where a fully percolated KB network is well constructed [Fig. 4]. For the L_2-based KB dispersions (decanol/water ratio >0.3), G_0 increases by one decade and almost remains independent of the decanol/water ratio. This implies that hydrophobic KB agglomerates and "encapsulates" in the organic droplets of the W/O microemulsion so that any increase in the decanol content does not alter the rheological behavior. The inset optical photograph (right) is evident to the equilibrium microstructure of KB in W/O microemulsions where the KB agglomerates are encapsulated in isolated domains where the KB network loses its percolation identity.

It is well stated that the impedance spectra and extrapolated electrical conductivity of dispersions are very sensitive to the microstructure.[23] The equilibrium microstructure of KB dispersions can be revealed by monitoring the electrochemical impedance spectra, represented by Nyquist plots (variation of the imaginary part of impedance Z'' versus the real component Z') as shown in Fig. 5. In general, all the KB dispersions show semicircle Nyquist plots implying the conductive nature of dispersions at the 2 wt% KB content, consistent with previous findings for CB dispersions.[5] For each dilution line (i.e., at constant Triton concentration), the semicircles get narrower as the decanol concentration increases, implying the increased electrical conductivity. To better account for the effect of decanol on the electrical behavior of dispersions, the Nyquist plots were fitted by previously proposed equivalent circuit[5] using EC-Labs software

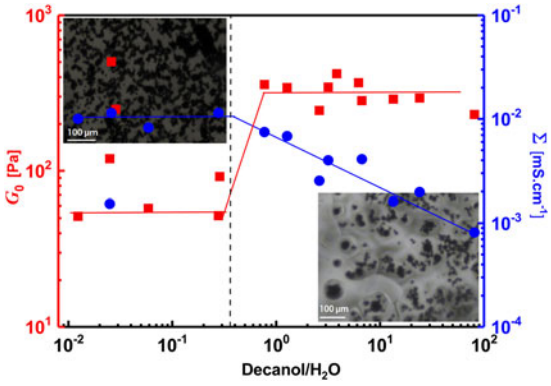


FIG. 5. Impedance spectra, represented by Nyquist plots (imaginary Z'' versus real Z' component of impedance), of 2 wt% KB in L_1 (circles) and L_2 (squares) microemulsions at rest, at 25 °C (at 100 mV).

(Bio-Logic Science-Instruments) to extrapolate the electrical conductivity (Σ) of dispersions.

As can be seen from Fig. 4, the L_1-based KB dispersions show higher electrical conductivity than those prepared in the L_2 phase. In addition, the conductivity of L_2-based KB dispersions is very sensitive to decanol addition and exhibits a monotonic decrease as the decanol concentration increases. This behavior may be attributed to the isolation of KB aggregates due to the decrease of the number density of conductive branches when the decanol concentration increases. On the other hand, O/W microemulsions stabilize the KB dispersions and the percolated network is still constructed.

In conclusion, the dispersion of 2 wt% KB in the O/W microemulsion system (at 2–4 wt% decanol) showed the optimal rheological (less rigidity) and electrical (higher conductivity) properties that render them adequate conductive substrates to formulate electrode slurries with sufficient colloidal stability.

D. Dispersions of CB in microemulsions: effect of shear flow

Since the linear viscoelastic rheology revealed the equilibrium microstructure of KB dispersions, it worth examining their flow behavior under destructive conditions to account for probable shear-induced structural transitions. The steady-shear rheology represented by the variation of steady viscosity (η) with shear rate is depicted in Fig. 6 for two selected KB dispersions in L_1 and L_2 phases. In general, the two KB dispersions show a non-Newtonian behavior with yield stress where the dispersions exhibit two shear-thinning regimes at low and high shear rates separated by a shear-thickening region over intermediate rates. Such a complex rheological behavior had previously been reported for analogous dispersions of CB and nanofibers.[5,24] In terms of shear-induced structural transitions, the first shear-thinning is

https://doi.org/10.1557/jmr.2017.451 Published online by Cambridge University Press

mainly attributed to the breaking up of the percolated network into small KB aggregates so that the viscosity tremendously decreases. As the shear rate increases, the anisometric KB aggregates erode under flow, showing leveling-off (shear-thickening) at intermediate rates. Upon further increase of the shear rate, the aggregates align with the flow showing the second shear-thinning. By comparison, the L_1-based dispersion shows a shear-thickening region at relatively higher shear rates than the L_2 dispersion. This implies the strength of the percolated network of KB in the L_1 phase.

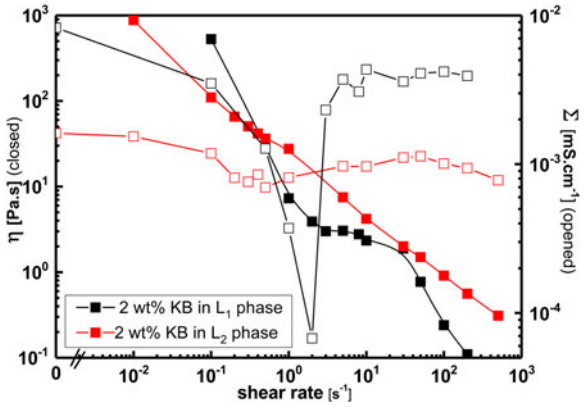


FIG. 6. Variation of steadyi viscosity (η) and electrical conductivity (Σ) with shear rate for 2 wt% KB dispersions in L_1 (28 wt% Triton X100, 4 wt% decanol, and 68 wt% H_2O) and L_2 (28 wt% Triton X100, 67 wt% decanol, and 5 wt% H_2O) phases.

Simultaneous measurements of the electrical conductivity under shear flow support the trend of viscosity with shear rate. As can be seen from Fig. 6, the KB dispersion in the L_1 phase has higher electrical conductivity than its analogous in the L_2 phase over the extended shear rate. In line with the three-regime flow curve, the electrical conductivity first decreases with the shear rate showing a minimum over intermediate shear rate in tandem with the shear-thickening region. Further increase of the shear rate results in increasing of the electrical conductivity. It should be noted that conductivity minimum is much more pronounced for the KB

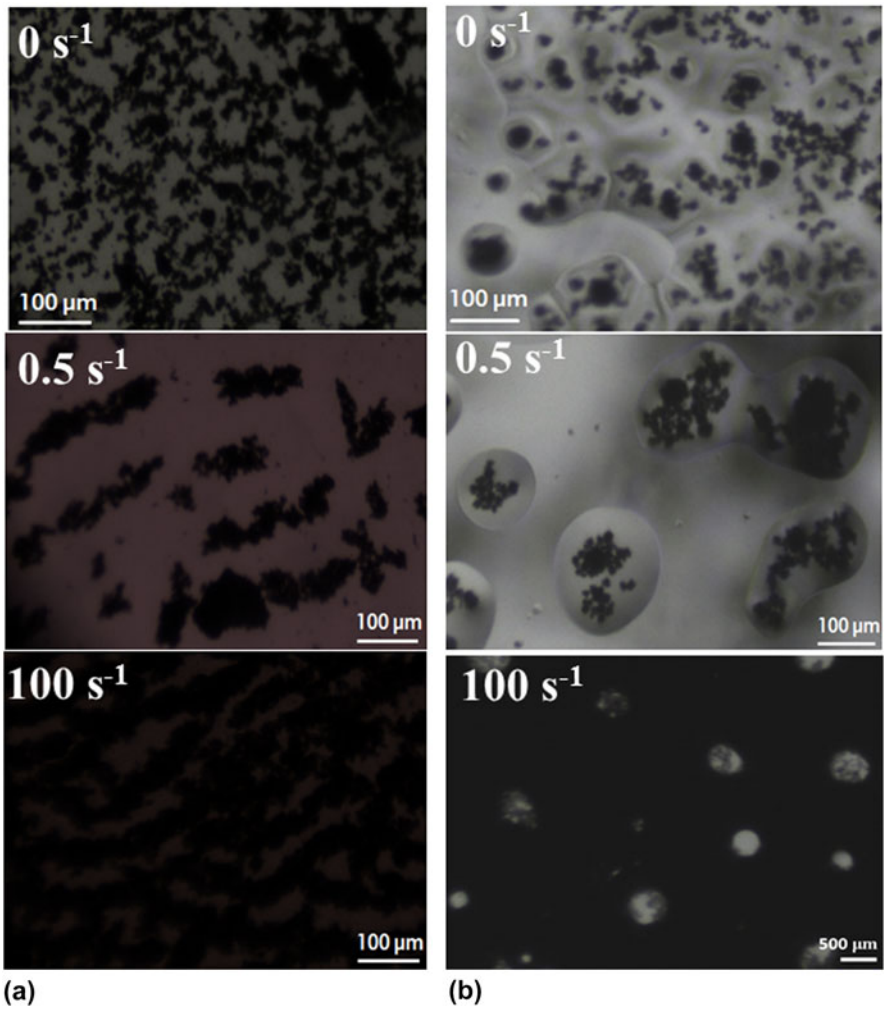


FIG. 7. Optical photographs of KB dispersions in (a) L_1 and (b) L_2 microemulsions at rest (shear rate = 0 s^{-1}) and flow conditions (shear rates = 0.5 and 100 s^{-1}).

https://doi.org/10.1557/jmr.2017.451 Published online by Cambridge University Press

dispersion in the L_1 phase than the dispersion in the L_2 phase.

The optical inspection of the KB dispersions under shear flow introduces direct evidence for the structural transitions. Figure 7 represents the textures of two KB dispersions in L_1 and L_2 phases. At rest (0 s^{-1}), the L_1-based dispersion shows a percolated KB network that undergoes shear-induced breaking up into anisometric aggregates at 0.5 s^{-1} [Fig. 7(a)], in agreement with the decrease in viscosity and electrical conductivity as discussed above. At higher shear rates (100 s^{-1}), the anisometric aggregates come in contact and align under flow leading to recovered electrical conductivity. On the other hand, the L_2-based dispersion [Fig. 7(b)] lacks the three-dimensional percolated network and the KB aggregates seem to be encapsulated in the large droplets at rest (0 s^{-1}). Under shear flow, the droplets and encapsulated KB aggregates become smaller as the shear rates increase.

IV. CONCLUSION

In this article, we demonstrate a comparative study for the rheological and electrical properties of CB (KB) dispersions in the oil-in-water (O/W) and water-in-oil (W/O) microemulsion systems composed of a nonionic surfactant (Triton X100), decanol, and water. Besides the traditional rheology, simultaneous measurements of the impedance spectra (rheo-electrical) and optical texture (rheo-microscopy) of the KB dispersions at equilibrium and under shear flow proved to be powerful techniques to elucidate the equilibrium microstructure and shear-induced structural transitions in CB dispersions.

The percolated KB dispersions (at 2 wt%) in O/W microemulsions at relatively low (2–4 wt%) decanol concentration exhibited optimal rheological (low plateau modulus, i.e., less rigidity) and electrical (higher electrical conductivity) properties with enhanced colloidal stability than those prepared in W/O microemulsions or in micellar systems of Triton X100 (decanol-free).

The shear-induced structural transitions reflected by the three-regime (thinning-thickening-thinning) flow curve and inverted-bell conductivity curve of KB dispersions were clearly discussed, for the first time, in light of the visual inspection of textures by rheo-microscopy.

REFERENCES

1. S. Flandrois and B. Simon: Carbon materials for lithium-ion rechargeable batteries. *Carbon* **37**(2), 165 (1999).
2. M. Armand and J-M. Tarascon: Building better batteries. *Nature* **451**(7179), 652 (2008).
3. Q. Zhang, E. Uchaker, S.L. Candelaria, and G. Cao: Nanomaterials for energy conversion and storage. *Chem. Soc. Rev.* **42**(7), 3127 (2013).
4. F. Yao, D.T. Pham, and Y.H. Lee: Carbon-based materials for lithium-ion batteries, electrochemical capacitors, and their hybrid devices. *ChemSusChem* **8**(14), 2284 (2015).
5. M. Youssry, L. Madec, P. Soudan, M. Cerbelaud, D. Guyomard, and B. Lestriez: Nonaqueous carbon black suspensions for lithium-based redox flow batteries: Rheology and simultaneous Rheo-electrical behavior. *Phys. Chem. Chem. Phys.* **15**(34), 14476 (2013).
6. T. Amari and K. Watanabe: Flow properties and electrical conductivity of carbon black–linseed oil suspension. *J. Rheol.* **34**(2), 207 (1990).
7. D.B. Genovese: Shear rheology of hard-sphere, dispersed, and aggregated suspensions, and filler-matrix composites. *Adv. Colloid Interface Sci.* **171–172**, 1 (2012).
8. S-P. Rwei, F-H. Ku, and K-C. Cheng: Dispersion of carbon black in a continuous phase: Electrical, rheological, and morphological studies. *Colloid Polym. Sci.* **280**(12), 1110 (2002).
9. Z. Chang, Y. Yang, M. Li, X. Wang, and Y. Wu: A hybrid of CoOOH nanorods with carbon nanotubes as a superior positive electrode material for supercapacitors. *J. Mater. Chem. A* **2**(103), 10739 (2014).
10. J-Y. Luo, W-J. Cui, P. He, and Y-Y. Xia: Raising the cycling stability of aqueous lithium-ion batteries by eliminating oxygen in the electrolyte. *Nat. Chem.* **2**(9), 760 (2010).
11. L. Madec, M. Youssry, M. Cerbelaud, P. Soudan, D. Guyomard, and B. Lestriez: Surfactant for enhanced rheological, electrical, and electrochemical performance of suspensions for semisolid redox flow batteries and supercapacitors. *ChemSusChem* **80**(2), 396 (2015).
12. D.F. Evans, D.J. Mitchell, and B.W. Ninham: Oil, water, and surfactant: Properties and conjectured structure of simple microemulsions. *J. Phys. Chem.* **90**(13), 2817 (1986).
13. K. Shinoda and B. Lindman: Organized surfactant systems: Microemulsions. *Langmuir* **3**(2), 135 (1987).
14. H.L. Rosano, J.L. Cavallo, D.L. Chang, and J.H. Whittam: Microemulsions: A commentary on their preparation. *J. Soc. Cosmet. Chem.* **39**(3), 201 (1988).
15. A.M. Cazabat, D. Langevin, J. Meunier, and A. Pouchelon: Critical behavior of microemulsions. *Adv. Colloid Interface Sci.* **16**, 175 (1982).
16. M.O. Iwunze, A. Sucheta, and J.F. Rusling: Bicontinuous microemulsions as media for electrochemical studies. *Anal. Chem.* **62**(6), 644 (1990).
17. J.F. Rusling: Electrochemistry in micelles, microemulsions, and related organized media. In *Electroanalytical Chemistry*, Vol. **18**, A.J. Bard, ed., (Marcel Dekker, New York, 1994); pp. 1–88.
18. C. La Mesa, G.A. Ranieri, and M. Terenzi: Phase diagram of the system water–Triton TX 100–decanol: A thermodynamic study. *Colloids Surf.* **42**(1), 59 (1989).
19. G.G. Warr: Shear and elongational rheology of ternary microemulsions. *Colloids Surf., A* **103**(3), 273 (1995).
20. G. Sharma, K. Wilson, C.F. van der Walle, N. Sattar, J.R. Petrie, and M. Kumar: Microemulsions for oral delivery of insulin: Design, development and evaluation in streptozotocin induced diabetic rats. *Eur. J. Pharm. Biopharm.* **76**(2), 159 (2010).
21. D.P. Acharya and P.G. Hartley: Progress in microemulsion characterization. *Curr. Opin. Colloid Interface Sci.* **17**(5), 274 (2012).
22. M. Youssry, F. Kamand, M.I. Magzoub, and M.S. Nasser: Aqueous dispersions of carbon blacks and their hybrid with carbon nanofibers. *J. Colloid Interface Sci.* (submitted).
23. J. Mewis, L.M. de Groot, and J.A. Helsen: Dielectric behaviour of flowing thixotropic suspensions. *Colloids Surf.* **22**(2), 271 (1987).
24. M. Youssry, D. Guyomard, and B. Lestriez: Suspensions of carbon nanofibers in organic medium: Rheo-electrical properties. *Phys. Chem. Chem. Phys.* **17**(48), 32316 (2015).

https://doi.org/10.1557/jmr.2017.451 Published online by Cambridge University Press